The Dangers of Abatement Procrastination in a Tipping Climate

Andrea Titton*

April 15, 2024

Abstract

This paper investigates the role of non-linear tipping points in determining optimal abatement policies. To do so, I introduce a stylised ice-albedo tipping point in the climate dynamics and study the consequences this has in determining optimal emissions in a dynamic stochastic general equilibrium model. In line with recent evidence, I assume that climate change hinders economic growth. I show that the presence of a tipping point prescribes ambitious abatement policies, not only in scope but, crucially, in timing. Finally, by comparing the model with the widely used stochastic tipping model, I show that in the latter abatement is slower and similar to a model with fast temperature growth but no tipping. This casts some doubts on the appropriateness of using stochastic tipping as an approximation for tipping points.

*Faculty of Economics and Business, University of Amsterdam (a.titton@uva.nl). I thank my supervisors Florian Wagener and Cees Diks for the patient guidance on this paper. I also thank the CeNDEF group and the Quantitative Economics section at the University of Amsterdam for helpful comments throughout the many seminars. Finally, I thank the attendees of the SEEMS/ASF seminar series for their feedback.

As the world temperature rises, due to carbon dioxide (CO2) emissions from human economic activities, the risk of tipping points in the climate system becomes more concrete (Ashwin and Von Der Heydt, 2020; Sledd and L'Ecuyer, 2021). This risk affects the trade-off between the economic gains from emissions and the damages such emissions impose on the economy. In this paper, I study the relationship between the presence of a tipping point and the optimal abatement of emissions. To do so, I solve a social-planner integrated assessment model with a stylised ice-albedo feedback in the climate dynamics (Hogg, 2008; Ashwin et al., 2012) and study the effect this has on optimal abatement policies. The tipping point affects temperature dynamics, and as a consequence optimal emissions, in three ways. First, it introduces a non-linear increase in temperature. Second, it makes positive temperature shocks more persistent than negative ones. Third, it introduces a jump in the abatement necessary to revert temperatures to the pre-tipping-point level. I show that, when tipping points are present, optimal abatement is more ambitious in scope and timing

The importance of modelling precise climate dynamics and tipping points when determining optimal emission paths has been increasingly recognised in economics (Van den Bremer and Van der Ploeg, 2021; Dietz et al., 2021, 2020; Taconet, Guivarch and Pottier, 2021; Lontzek et al., 2015). Previous approaches have mostly focused on the stochastic nature of tipping points, by modelling temperature dynamics (Dietz et al., 2021) or damages (Lontzek et al., 2015) as jump processes, with arrival rates increasing in emissions. Yet, many tipping points in the climate system are caused by bifurcations (Ashwin and Von Der Heydt, 2020; Ashwin et al., 2012). In this paper, I show that introducing this class of tipping points in an integrated assessment model yields similar predictions in terms of aggregate emissions, but prescribes much steeper reduction of emissions to keep the risk of tipping low.

To tease out this difference, I study an AK-model in which increases in temperature, beyond pre-industrial levels, reduce economic growth (as in Pindyck and Wang (2013) and Hambel, Kraft and Schwartz (2021)). This modelling choice, as opposed to having temperatures wipe-out a fraction of the capital stock, as in Nordhaus (2014; 2008; 2017), is motivated by recent evidence on the role of temperature in reducing economic growth and productivity (Burke, Hsiang and Miguel, 2015; Dietz and Lanz, 2019).

1 Climate Model

1.1 CO_2 concentration and carbon sinks

The average atmospheric carbon dioxide (CO_2) concentration, in parts-per-million by volume (p.p.m.) at time t, is denoted by M. In the model, CO_2 concentration dynamics are determined by two processes: first, emissions by human activity E, in Gt s^{-1}, and, second, a decay into natural sinks, which happens at a rate of δ_m per s. To model the reduced capacity of natural sinks to remove CO_2 from the atmosphere, we assume that the decay rate falls in the quantity of carbon dioxide already stored in the natural sinks N, in Gt. To make this relationship explicit, I write $\delta_m(N)$. This also implies that the carbon stored in natural sinks evolves as

$$\xi \, \mathrm{d}N = \delta_m(N) M \, \mathrm{d}t, \tag{1}$$

where ξ is a factor converting Gt of CO_2 to atmospheric p.p.m.. Putting these two flows together, we can write CO_2 concentration dynamics as

$$\mathrm{d}M = \left(\xi E - \delta_m(N) M\right) \mathrm{d}t, \tag{2}$$

where the level of emissions E is determined endogenously by economic activity.

The aim of the paper is to look at optimal abatement strategies. To make the relationship between the abatement strategy and the climate model more transparent, I rewrite the level of emissions E in deviation from a business-as-usual scenario E^{b}. Furthermore, I normalise these two quantities with respect to the corresponding level of CO_2 concentration, M and M^{b}. To do so, let γ^{b} be the expected observed growth rate of carbon concentration, in a business-as-usual scenario, such that $\mathrm{d}M^{\mathrm{b}} = M^{\mathrm{b}} \gamma^{\mathrm{b}} \, \mathrm{d}t$. Using the CO_2 concentration dynamics (2) we obtain

$$\gamma^{\mathrm{b}} = \frac{\xi E^{\mathrm{b}} - \delta_m(N^{\mathrm{b}}) M^{\mathrm{b}}}{M^{\mathrm{b}}}, \tag{3}$$

where N^{b} is the quantity of CO_2 sequestered in natural sinks, in a business-as-usual scenario. The quantities E^{b}, M^{b}, and N^{b} are all calibrated using the SSP5 scenarios (Intergovernmental Panel On Climate Change, 2023), such that γ^{b} is an time-varying exogenous parameter. Using this, we can rewrite the societal abatement strategy as a deviation from the business-as-usual growth rate. Let α be such abatement strategy, then equation (2) can be rewritten as

$$\mathrm{d}m := \frac{\mathrm{d}M}{M} = \left(\gamma^{\mathrm{b}} - \alpha\right) \mathrm{d}t, \tag{4}$$

where m denotes the logarithm of the CO_2 concentration, $\log M$. Rewriting the dynamics as in equation (2) we rephrase the problem from optimal emissions to optimal abatement, vis-à-vis the business-as-usual scenario, which allows us to simplify exposition and to compare more effectively different policy scenarios. Yet, at time it is interesting to link a given abatement policy α back to emissions. To do so, I introduce the emission reduction rate ε, implicitly defined as

$$E = (1 - \varepsilon(\alpha))\, E^{\mathrm{b}}, \tag{5}$$

which is the fraction of emission society is abating compared to the business-as-usual scenario.

1.2 Temperature

Global mean surface temperature T is modelled using a stylised Budyko–Ghil–Sellers energy balance model (Hogg, 2008; Ashwin and Von Der Heydt, 2020). Earth's radiating balance, in its simplest form, prescribes that an equilibrium temperature $\bar{T}$, in K, is determined by equating incoming solar radiation S, in Wm^{-2}, with outgoing longwave radiations $\eta\sigma\bar{T}^4$, where $\sigma = 5.7 \times 10^{-8}$ $\mathrm{Wm}^{-2}\mathrm{K}^{-4}$ is the Stefan-Boltzmann constant and η is an emissivity rate. Due to the presence of greenhouse gasses, certain wavelengths are scattered and, hence, not emitted, which introduces an additional radiative forcing G, in Wm^{-2}, which yields the balance equation $S = \eta\sigma\bar{T}^4 - G$. In this paper, we focus on the role of increased CO_2 concentration M compared to pre-industrial levels M^{p}, as opposed to other greenhouse gases, hence we can decompose the greenhouse radiative forcing term G into a constant component G_0 and a component which depends on the steady state level of CO_2 concentration in the atmosphere $\bar{M}$ with respect to the pre-industrial level M^{p}, such that $G = G_0 + G_1 \log(\bar{M}/M^{\mathrm{p}})$.

In addition to these forces, to study the role of tipping points, I introduce the effects of land ice albedo on the radiation balance (as done in Ghil and Childress (2011); Dijkstra and Viebahn (2015)). In particular, as temperatures rise, the area of ice caps, glaciers, and sea ice shrinks, which in turn reduces the planetary albedo $\lambda(T)$, that is, the fraction of solar radiation reflected by earths' surface. Hence, the solar radiation which contributed to warming is a fraction of the total incoming solar radiation $S = S_0\big(1 - \lambda(T)\big)$. This effect is modelled by letting the planetary albedo transition from a high level λ_1 to a lower level

$(\lambda_1 - \Delta\lambda)$ via a sigmoid transition function

$$\sigma(T) = \frac{1}{1 + \exp(T_i - T)} \tag{6}$$

where T_i is a calibrated inflection point. Under this specification, the albedo coefficient can be written as a function of temperature (Figure 1)

$$\lambda(T) = \lambda_1 - (1 - \sigma(x))\Delta\lambda. \tag{7}$$

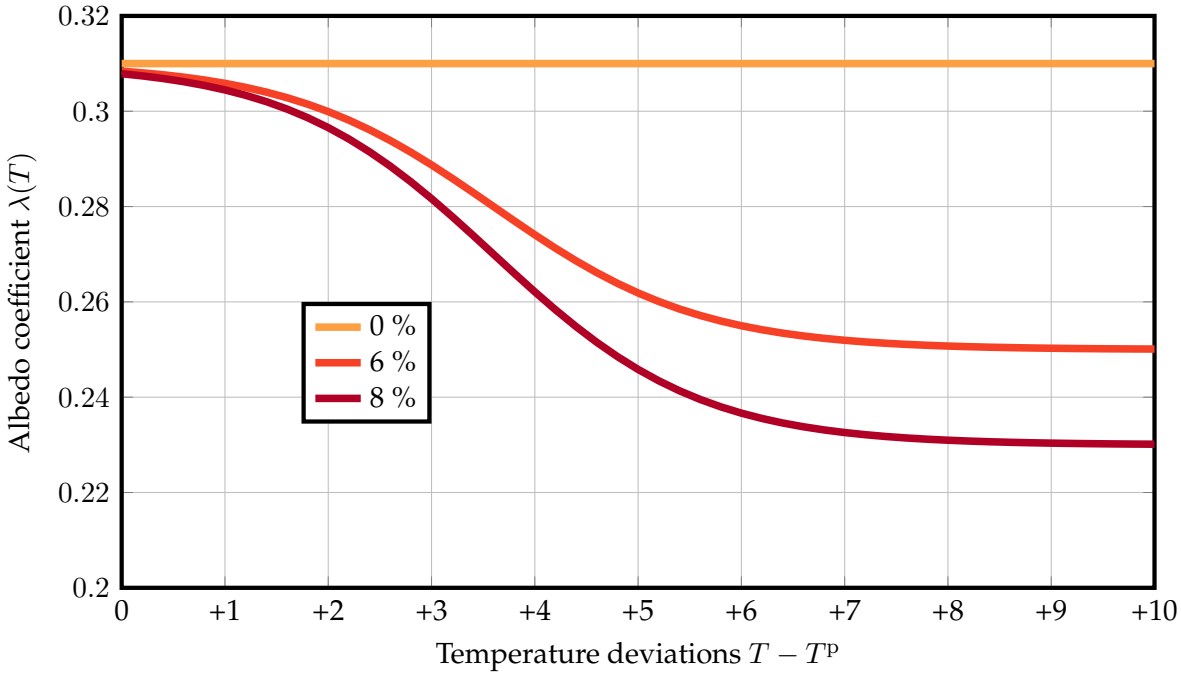

Figure 1: Albedo coefficient $\lambda(T)$ for different parametrisations of the albedo loss $\Delta\lambda$.

It is the important to stress that the function λ (7) is a highly stylised average model for a complex and spatially heterogeneous process, which, in turn, puts a lot of uncertainty around the parameters T_i and $\Delta\lambda$.

Equating incoming solar radiation, net of the albedo effect, and outgoing longwave radiation, net of the greenhouse gas effect, we obtain the energy balance condition

$$S_0\big(1 - \lambda(\bar{T})\big) = \eta\sigma\bar{T}^4 - G_0 - G_1 \log(\bar{M}/M^{\mathrm{p}}). \tag{8}$$

To study deviations from radiative balance (8), we define the contribution of tempera-

ture to forcing

$$\mu_T(T) \coloneqq S_0\big(1 - \lambda(T)\big) - \eta\sigma\bar{T}^4 \tag{9}$$

and that of log-carbon concentration

$$\mu_m(m) \coloneqq G_0 + G_1\big(m - m_p\big), \tag{10}$$

and notice that we can rewrite radiative balance (8) as $\mu_T(\bar{T}) + \mu_m(\bar{m}) = 0$. Then we assume that temperature dynamics are given by

$$\epsilon \, \mathrm{d}T = \Big(\mu_T(T) + \mu_m(m)\Big) \, \mathrm{d}t + \sigma_x \, \mathrm{d}w_2 \tag{11}$$

where ϵ, in $\mathrm{Jm}^{-2}\mathrm{K}^{-1}$, is the thermal inertia and w^T is a Wiener process.

1.3 Ice-albedo Feedback and Tipping Points

The presence of the ice-albedo feedback effect $\lambda(T)$ can introduce tipping points in the temperature dynamics. To illustrate this, Figure 2 depicts the values of temperature $\bar{T}$ and logarithmic carbon concentration $\bar{m}$, for which the system is in radiative balance, $\mu_T(\bar{T}) + \mu_m(\bar{m}) = 0$, with three different potential albedo losses $\Delta\lambda$. For no albedo loss ($\Delta\lambda = 0\%$), as the logarithm of carbon concentration increases, equilibrium temperatures rise linearly. As the albedo loss increases ($\Delta\lambda = 6\%$), an equivalent increase in carbon concentration, yields larger and non-linear increases in temperature. Past a certain threshold, the system undergoes a bifurcation, and, for some levels of carbon concentration, one additional stable equilibrium arises ($\Delta\lambda = 8\%$). This new equilibrium represents a situation in which a significant fraction of the ice coverage has melted and cannot reform naturally, without large decreases in carbon concentration. For example, consider the carbon concentration level $M = 610$ in Figure 2. For $\Delta\lambda = 6\%$, the only temperature that yields radiative balance, in deviation from pre-industrial level is approximately $+3.5°$. For $\Delta\lambda = 8\%$, at the same level of carbon concentration, radiative balance is achieved at both $+4°$and $+7.5°$.

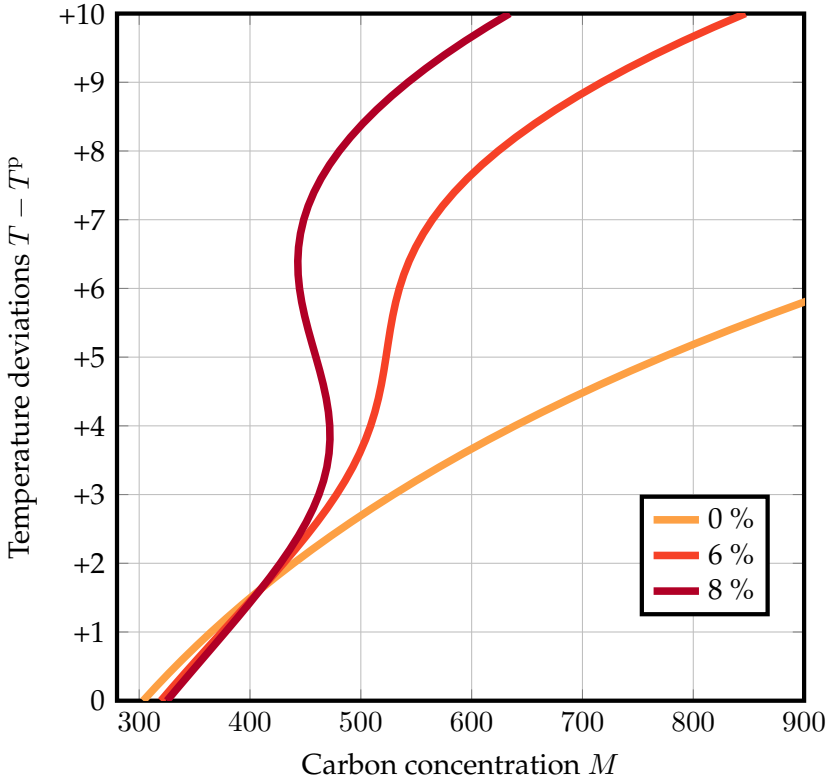

Figure 2: Nullclines of the dynamics $\{(T, M) : \dot{T} = 0\}$ for different parametrisations of albedo loss $\Delta\lambda$.

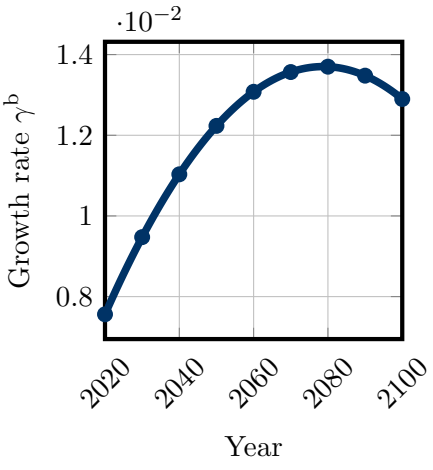

Figure 3

The presence of a bifurcation induced by the ice-albedo feedback has strong implications for the dynamics. To illustrate this, we can calibrate the model using the *SSP5 - Baseline* scenario (Kriegler et al., 2017) as a business-as-usual benchmark. This scenario describes an energy intensive future, in which fossil fuel usage develops rapidly and little to no abatement takes place. The growth rate of carbon concentration γ^{b} (3) implied by the *SSP5 - Baseline* is plotted in Figure 3 (the calibrated parameters can be found in B).

Using the calibrated growth rate of carbon concentration γ^{b}, I simulate the business-as-usual $\alpha = 0$ path of temperature and carbon concentration implied by the dynamics (4) and (11). With no ice-albedo feedback (left panel of Figure 4), as expected, temperature grows with the logarithm of carbon concentration and the model, despite its simplicity, tracks well the *SSP5 - Baseline* temperature projections. Under a larger albedo loss (right

panel of Figure 4) keeping the same emissions, the temperature exhibits a very different path. After passing a critical threshold, the temperature converges rapidly to a second steady state. Crossing this tipping point represents a large threat to the economy. First, an acceleration of temperature growth causes large economic damages. Second, removing the emitted carbon that triggered the tipping point is not sufficient to revert back to the pre-tipping equilibrium. These two factors impose a discontinuity in the externality of emissions: the ton of carbon that triggers a transition is discontinuously more damaging than the previous one.

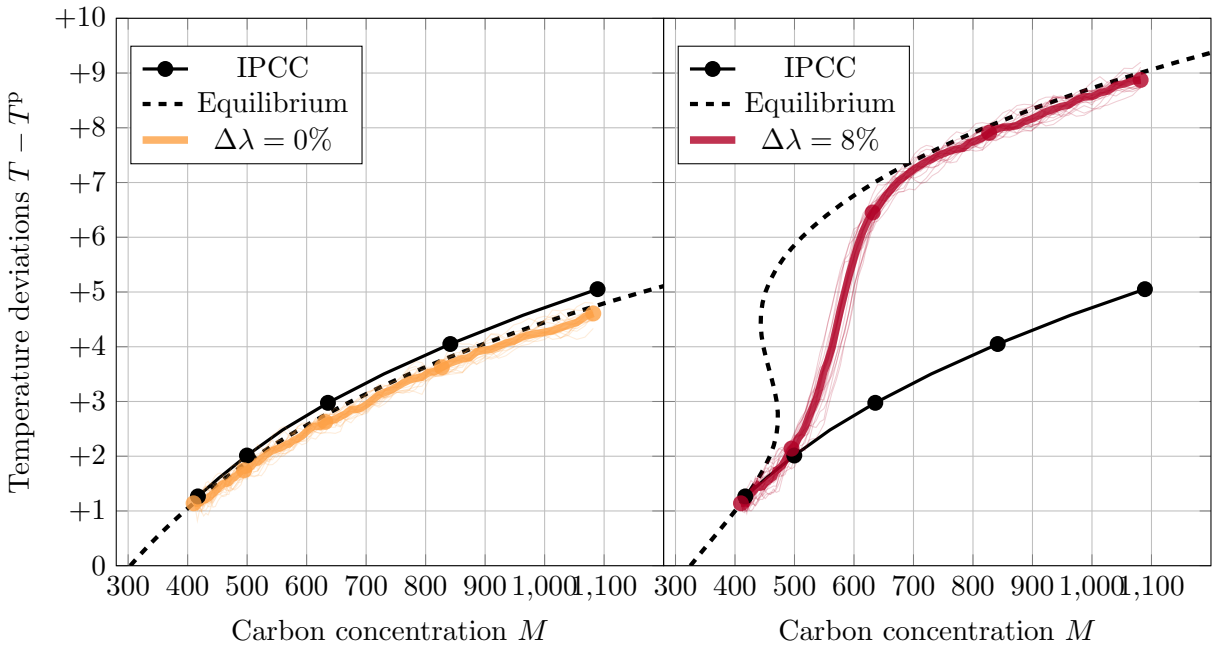

Figure 4: Business as usual path of temperature with small (left) and large (right) albedo loss. Each marker represents the temperature every 20 years, starting from 2020. In black, the *SSP5 - Baseline* model.

1.4 Critical Slowdown and Early Warning Signals

Another crucial difference between the climate dynamics in the presence of a tipping point, vis-à-vis those modelled with a jump process (e.g. Dietz et al. 2021; Hambel, Kraft and Schwartz 2021) is the presence of critical slowdown: as we approach the tipping point, large temperature deviation shocks persist for longer, as ice struggles

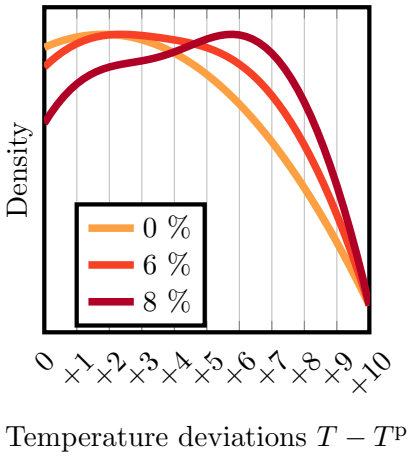

Figure 5: Density of temperature shocks at $M = 600$.

to reform. To illustrate this effect, Figure 5 shows the density of temperature as carbon concentration approaches the tipping point (derived in Appendix A). For larger levels of albedo loss, large deviations of temperature are more persistent, hence more time are spent in a high temperature regime. This has two relevant implications for optimal emissions. First, it can act as an early warning signal; if one is uncertain about the size of the albedo loss, long periods of high temperature can be used to infer that the loss is high and the system is approaching the tipping point. Second, such repeated and persistent periods of high temperatures generate large economic damages.

2 Economy

In the model, the economy interacts with the climate in two ways. First, the economy alters climate dynamics by emitting carbon dioxide E as a by-product of output production Y. Second, as the climate changes and temperatures T rise, the rate of capital depreciation increases, thereby lowering economic growth. This is in line with recent empirical evidence on the role of temperature variations in lowering output growth (Dell, Jones and Olken, 2009; 2012)

As in Pindyck and Wang (2013) and Hambel, Kraft and Schwartz (2021), I assume output Y to be a linear function of capital K,

$$Y = AK, \tag{12}$$

where A denotes total factor productivity. Output can be used for investment I, abatement expenditures B, or consumption C

$$Y = I + B + C. \tag{13}$$

As in Nordhaus (1992; 2008), I assume abatement expenditures to be proportional to output Y and quadratic in the emission reduction rate ε (5), namely $B = \beta(\varepsilon)Y$ where

$$\beta(\varepsilon) = \frac{1}{2}\omega\varepsilon^2. \tag{14}$$

The function $\beta(\varepsilon)$ captures the idea that, at a time t, a marginal reduction in emissions, vis-

à-vis the business-as-usual scenario, becomes increasingly costly at a rate $\omega\varepsilon$. As time progresses, so does abatement technology and a given abatement objective becomes cheaper. We model this by letting the exogenous technological parameter ω decrease over time.

2.1 The Role of Climate Change

In the last 50 years, productivity in the agricultural sector, net of technological growth, has declined due to temperature increases (Dell, Jones and Olken 2009). Given the imperfect substitutability of food, resources have been diverted from other sectors towards agriculture which has increased the opportunity cost of capital investment in manufacturing and services. For a thorough treatment of this mechanic see Dietz and Lanz (2019). In this paper, I will abstract from the details of the mechanism but keep the role of temperatures in reducing capital growth rate and assume this to be the main damage deriving from climate change. In the model, capital depreciates at a rate $\delta_k + d(T)$ where δ_k is the depreciation rate of capital at pre-industrial temperature levels T^p and $d(T)$ is the damage function. Following Weitzman (2012), I assume the damage function to take the form

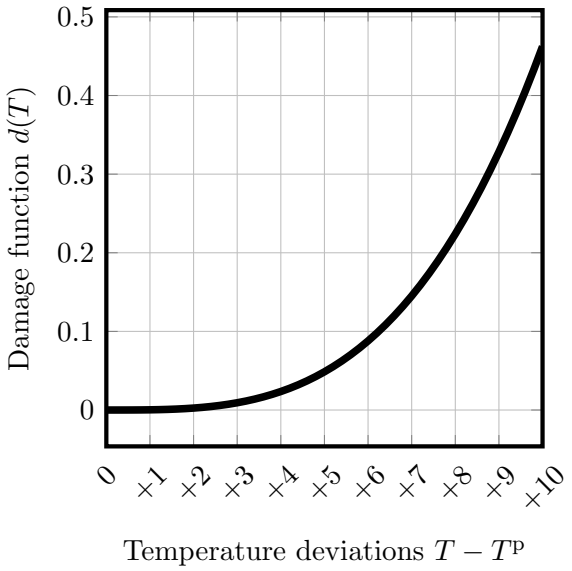

Figure 6: Calibrated damage function $d(T)$

$$d(T) = \xi(T - T^p)^{\upsilon}. \tag{15}$$

Finally, in investing and abating the economy incurs adjustment costs proportional to capital $\frac{\kappa}{2}\big(I + B\big)^2\sqrt{K}$. Putting this all together we obtain the evolution of capital

$$\mathrm{d}K = \left(I - (\delta_k + d(T))K - \frac{\kappa}{2}\Big(I + B\Big)^2\sqrt{K}\right)\mathrm{d}t + K\sigma_K\ \mathrm{d}w_2, \tag{16}$$

where w_2 is a Wiener process. As in the climate model, it is convenient to rewrite the

dynamics in terms of growth rates. Let k be $\log K$, then equation (16) can be rewritten as

$$\mathrm{d}k = \left(\frac{I}{K} - \delta_k - d(T) - \frac{\kappa}{2} \left(\frac{I}{K} + \frac{B}{K} \right)^2 \right) + \sigma_K \, \mathrm{d}w_2. \tag{17}$$

Using the abatement costs (14), the abatement expenditure to capital ratio can be written as

$$\frac{B}{K} = A\beta(\varepsilon). \tag{18}$$

Furthermore, letting

$$\chi \coloneqq \frac{C}{Y} = \frac{C}{K}\frac{1}{A} \tag{19}$$

be the consumption share of output we can write the investment to capital ratio, using the budget equation (13), as

$$\frac{I}{K} = A\Big(1 - \chi - \beta(\varepsilon)\Big). \tag{20}$$

These two equations allow us to rewrite the log-growth of capital $\mathrm{d}k$ (17), in terms of the consumption decision χ, the abatement decision α, via the emission reduction rate ε, temperature T, and technological progress, in production A and abatement ω,

$$\mathrm{d}k = \left(\overbrace{A(1-\chi) - \frac{\kappa}{2}A^2(1-\chi)^2 - \delta_k}^{\text{Endogenous economic growth}} - \underbrace{A\beta(\varepsilon)}_{\text{Abatement}} - \overbrace{d(T)}^{\text{Climate damages}} \right) \mathrm{d}t + \sigma_K \, \mathrm{d}w_2 \tag{21}$$

The last step is to link this back to log-output growth $\mathrm{d}y$. This is easily done by letting the productivity growth rate be defined as $\varrho \, \mathrm{d}t = \mathrm{d}\log A$ and, to simplify notation, grouping endogenous economic growth as

$$\phi(\chi) \coloneqq A(1-\chi) - \frac{\kappa}{2}A^2(1-\chi)^2, \tag{22}$$

we can write changes in log GDP as

$$\mathrm{d}y = \Big(\varrho + \phi(\chi) - \delta_k - A\beta(\varepsilon) - d(T) \Big) \, \mathrm{d}t + \sigma_K \, \mathrm{d}w_2. \tag{23}$$

3 Social Planner Problem

To derive the optimal abatement path and the social cost of carbon, I solve the problem of a social planner who derives utility from consumption, is risk averse, and discounts

the future. To disentangle the role of these two components I model the social planner as having Epstein-Zin preferences. Societal utility U at time t, given an abatement strategy α and a consumption schedule χ, is defined recursively by the integral equation as

$$U(t;\alpha(t),\chi(t)) = \mathbb{E}_t \int_t^\infty f\left(C(s), U(s;\alpha(s),\chi(s))\right)\, \mathrm{d}s \tag{24}$$

where $C(s) = \chi(s)Y(s)$ is the consumption path. Introducing the coefficient of relative risk aversion $\theta > 1$, elasticity of intertemporal substitution $\psi > 0$, and the discount rate ρ, the Epstein-Zin aggregator (Duffie and Epstein, 1992) is defined as

$$f(C,U) = \frac{\rho}{1-1/\psi}(1-\theta)U\left(\left(\frac{C}{((1-\theta)U)^{\frac{1}{1-\theta}}}\right)^{1-1/\psi} - 1\right). \tag{25}$$

Given the optimal abatement and consumption schedule α and χ, let the value function be defined recursively as

$$V_t(T,m,y) = \sup_{\chi,\alpha} \mathbb{E}_t \int_t^\infty f(C,V_s)\, \mathrm{d}s, \tag{26}$$

which satisfies the Hamilton-Jacobi-Bellman (HJB)

$$\begin{aligned} -\partial_t V_t = {} & f(C,V_t) + \partial_T V_t\ \mu(T,m) + \partial_m V_t\ (\gamma_t - \alpha) + \\ & \partial_y V_t\ \Big(\varrho + \phi(\chi) - \delta_k - A\beta(\varepsilon) - d(T)\Big) + \\ & \frac{\sigma_k^2}{2}\partial_y^2 V_t + \frac{\sigma_T^2}{2}\partial_T^2 V_t \end{aligned} \tag{27}$$

The HJB equation is then solved numerically to obtain the value function at time $t = 0$, V_0, and obtain optimal consumption and abatement schedules. The details of the numerical procedure are laid out in Appendix D and E.

4 Benchmark model: Stochastic Tipping

Before analysing optimal emission with tipping points, this section introduces a benchmark model with stochastic tipping. Hereafter, I refer to the model as *Stochastic Tipping model*. The Stochastic Tipping model is a widely used in the economic literature to approximate tipping points in the climate dynamics (e.g. Hambel, Kraft and Schwartz 2021). Comparing the model developed in this paper with the Stochastic Tipping model allows us to determine if and how the optimal abatement differ and, as a consequence, what the approximation misses.

To establish a meaningful benchmark, I will assume that the albedo is constant in temperature, namely $\lambda(T) = \lambda_1$, such that the contribution of temperature to forcing (9) is given by

$$\mu_T^{\mathrm{ST}}(T) \coloneqq S_0(1 - \lambda_{\mathbf{1}}) - \eta\sigma T^4. \tag{28}$$

The tipping point does not arise due to the albedo coefficient changing, but is modelled as a counting process N with arrival rate $\pi(T)$ and intensity $\Theta(T)$, both increasing in temperature. Intuitively, as temperature rises, the risk of tipping $\pi(T)$ and the size of the temperature increase $\Theta(T)$ grow. Then temperature dynamics in the Stochastic Tipping model follow

$$\epsilon \, \mathrm{d}T = \left(\mu_T^{\mathrm{ST}}(T) + \mu_m(m)\right) \mathrm{d}t + \sigma_x \mathrm{d}w^{\mathrm{ST}} + \Theta(T)\mathrm{d}N. \tag{29}$$

Following Hambel, Kraft and Schwartz (2021), the calibrated arrival rate and temperature increase are calibrated as

$$\pi(T) = -\frac{1}{4} + \frac{0.95}{1 + 2.8e^{-0.3325(T - T^{\mathrm{P}})}} \text{ and} \tag{30}$$

$$\Theta(T) = -0.0577 + 0.0568(T - T^{\mathrm{P}}) - 0.0029(T - T^{\mathrm{P}})^2. \tag{31}$$

5 Main Results

Figure (7) and (8) display the optimal path of net emissions E and carbon concentration M respectively in three scenario: an albedo loss $\Delta\lambda = 6\%$, in which there is no tipping point; a loss of $\Delta\lambda = 8\%$ in which there is a tipping point; the benchmark stochastic model. The optimal emissions fall rapidly in all three parametrisation, highlighting the importance of rapid abatement. Yet, optimal emission path in the benchmark Stochastic Tipping model resembles closely that of 6% the albedo loss. On the contrary, in the presence of a tipping point, that is, the 8% albedo loss, emissions fall more rapidly and abatement policies are more ambitious. This leads to much lower optimal long run carbon concentration, if there is a tipping point induced by the albedo effect. Using the Stochastic Tipping model as an approximation of a tipping point can lead to insufficiently ambitious abatement policies, both in scope and in timing.

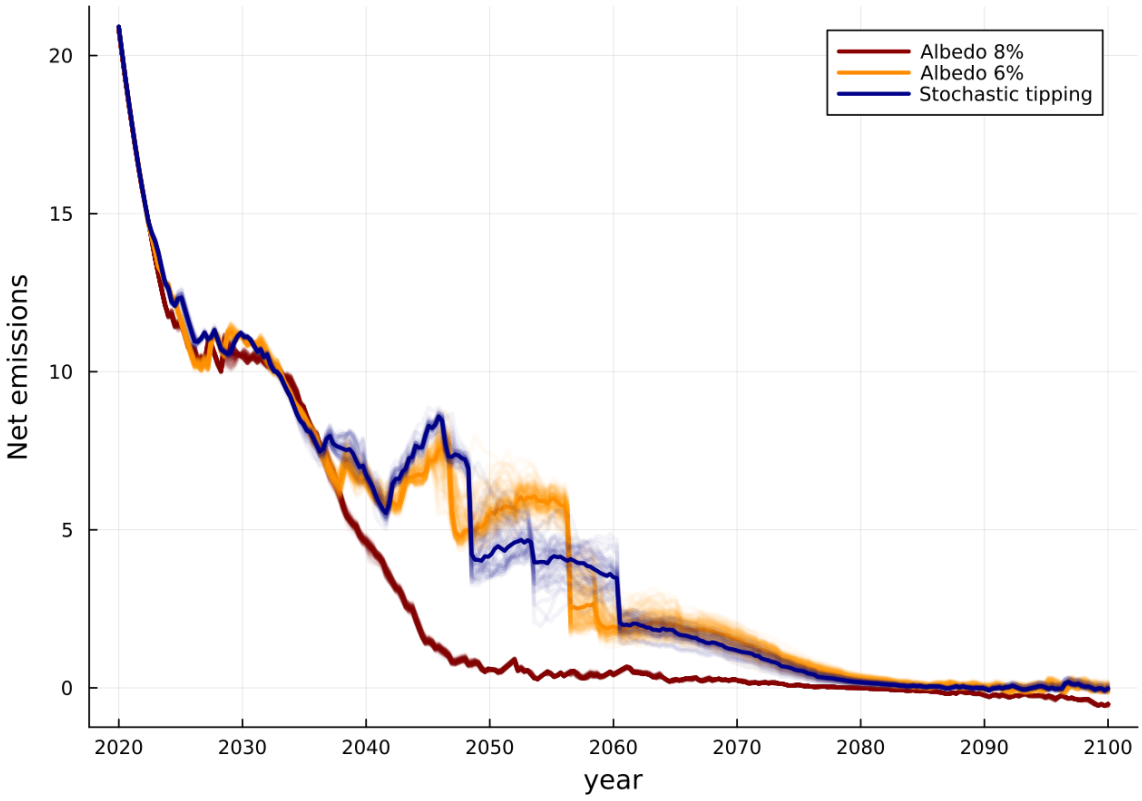

Figure 7: Optimal path of net emissions under the three model specifications, for 500 simulations.

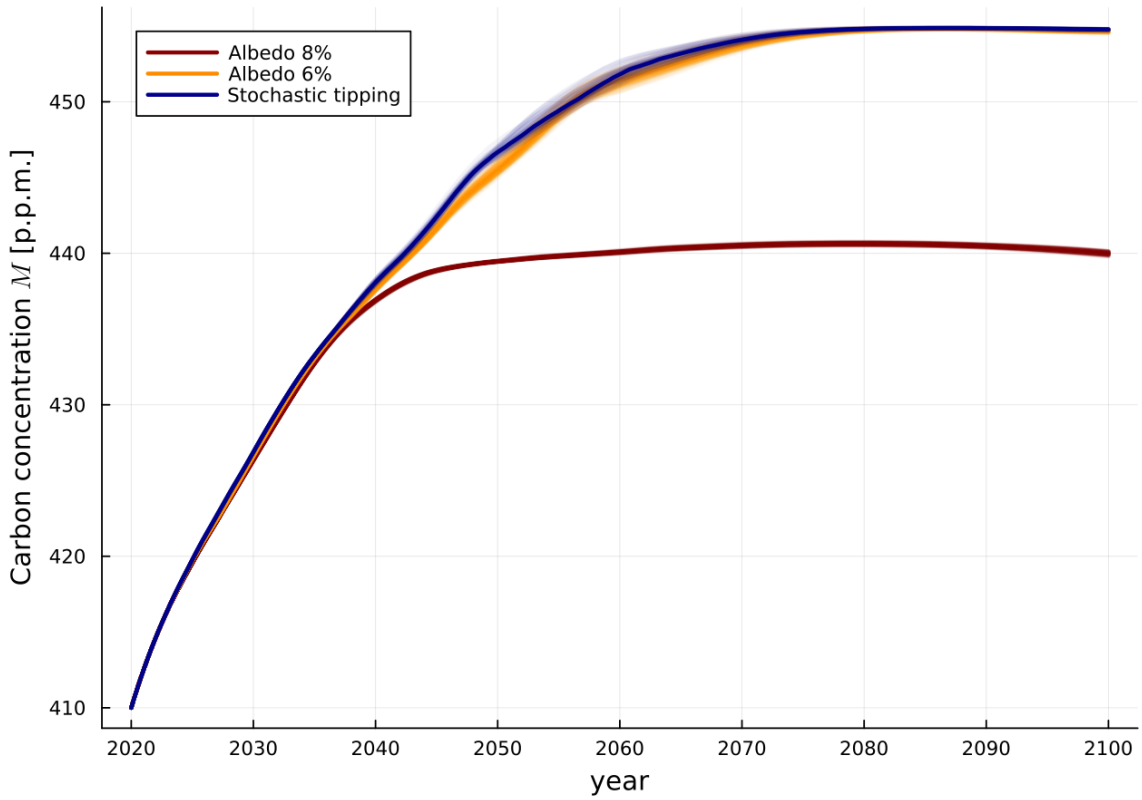

Figure 8: Optimal path of carbon concentration under the three model specifications, for 500 simulations.

Figure 9, shows the resulting optimal median path of GDP (solid line) and consumption (dashed line). GDP follows similar trajectories under all three specifications of climate dynamics, which suggests that the additional abatement expenditure in the case of 8% albedo loss, is fully compensated by reduced temperature damages. Yet, the amount of GDP consumed in the latter specification is lower than in the cases of 6% albedo loss and stochastic tipping, as more GDP is devoted to abatement.

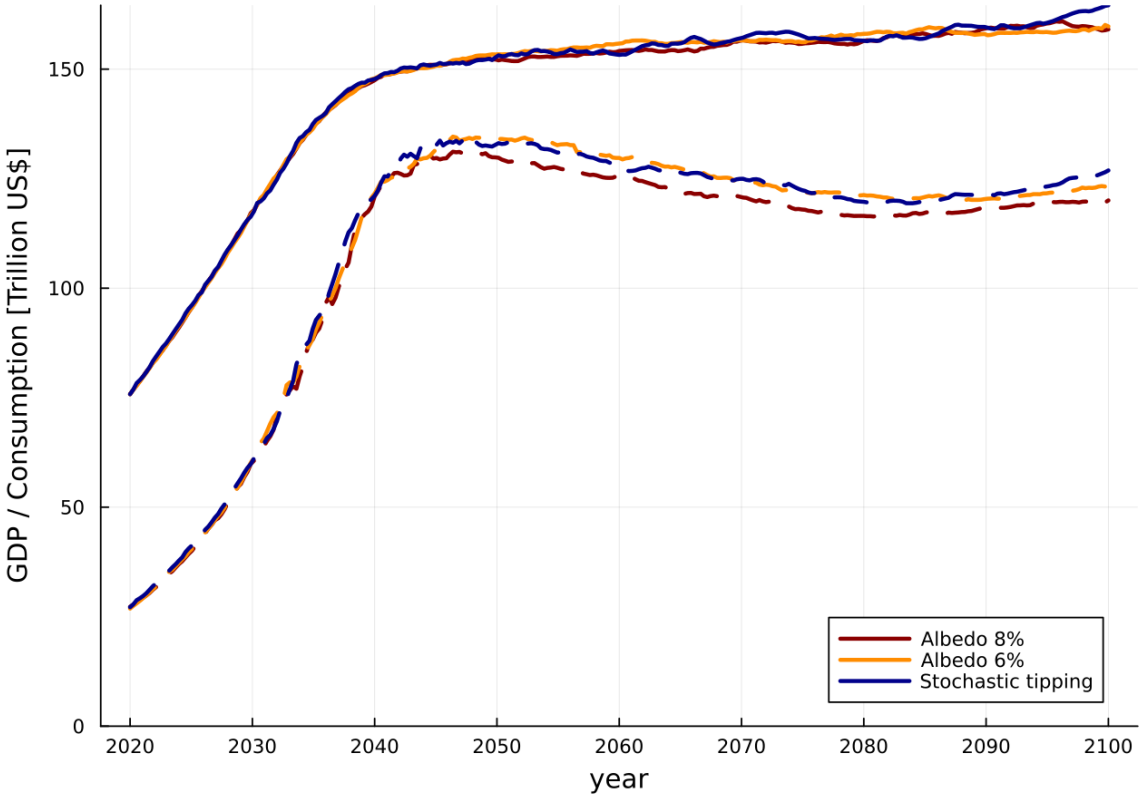

Figure 9: Optimal median path of GDP (solid) and consumption (dashed) under the three model specifications, for 500 simulations.

6 Conclusion

This paper studies the role of tipping points in determining optimal emissions. Building on the calibration by Hambel, Kraft and Schwartz (2021), I extend the climate dynamics to include a potential bifurcation induced by the loss in albedo due to the change in the area of ice caps, sea ice, and glaciers Ashwin et al. (2012); Ashwin and Von Der Heydt (2020). I show that, in the presence of tipping points, optimal abatement is more ambitious in scope and timing. In fact, early abatement is crucial to avoid long periods of exposure to tipping risk.

The model presented here represents an early and simplified analysis that can be ex-

tended in various directions. First, more work is needed to analytically link the risk of tipping and the optimal abatement strategy, in order to quantify precisely the role of higher order climate dynamics in determining the social cost of carbon. Second, the underlying assumption of the social planner's optimisation problem is that she knows the climate dynamics and the role of the ice-albedo feedback. Such an assumption calls for extending the analysis to a situation in which the magnitude of the albedo loss is not known and rather can be estimated using early warning signals. Yet, in the face of uncertainty, the optimal abatement policy derived in this paper serves as a good rule against the possible worst case scenario.

References

Ackerman, Frank, Elizabeth A. Stanton, and Ramón Bueno. 2013. "Epstein–Zin Utility in DICE: Is Risk Aversion Irrelevant to Climate Policy?" *Environmental and Resource Economics*, 56(1): 73–84.

Ashwin, Peter, and Anna S. Von Der Heydt. 2020. "Extreme Sensitivity and Climate Tipping Points." *Journal of Statistical Physics*, 179(5-6): 1531–1552.

Ashwin, Peter, Sebastian Wieczorek, Renato Vitolo, and Peter Cox. 2012. "Tipping points in open systems: bifurcation, noise-induced and rate-dependent examples in the climate system." *Philosophical Transactions of the Royal Society A: Mathematical, Physical and Engineering Sciences*, 370(1962): 1166–1184.

Burke, Marshall, Solomon Hsiang, and Edward Miguel. 2015. "Global non-linear effect of temperature on economic production." *Nature*, 527(7577): 235–239.

Crost, Benjamin, and Christian P. Traeger. 2013. "Optimal climate policy: Uncertainty versus Monte Carlo." *Economics Letters*, 120(3): 552–558.

Dell, Melissa, Benjamin F Jones, and Benjamin A Olken. 2009. "Temperature and Income: Reconciling New Cross-Sectional and Panel Estimates." *American Economic Review*, 99(2): 198–204.

Dell, Melissa, Benjamin F Jones, and Benjamin A Olken. 2012. "Temperature Shocks and Economic Growth: Evidence from the Last Half Century." *American Economic Journal: Macroeconomics*, 4(3): 66–95.

Dietz, Simon, and Bruno Lanz. 2019. "Growth and adaptation to climate change in the long run." IRENE Institute of Economic Research IRENE Working Papers 19-09.

Dietz, Simon, Frederick Van Der Ploeg, Armon Rezai, and Frank Venmans. 2020. "Are Economists Getting Climate Dynamics Right and Does it Matter?" *SSRN Electronic Journal*.

Dietz, Simon, James Rising, Thomas Stoerk, and Gernot Wagner. 2021. "Economic impacts of tipping points in the climate system." *Proceedings of the National Academy of Sciences*, 118(34): e2103081118.

Dijkstra, H. A., and Jan Viebahn. 2015. "Sensitivity and resilience of the climate system: A conditional nonlinear optimization approach." *Communications in Nonlinear Science and Numerical Simulation*, 22(1): 13–22.

Duffie, Darrell, and Larry G. Epstein. 1992. "Asset Pricing with Stochastic Differential Utility." *Review of Financial Studies*, 5(3): 411–436.

Epstein, Larry G., and Stanley E. Zin. 1989. "Substitution, Risk Aversion, and the Temporal Behavior of Consumption and Asset Returns: A Theoretical Framework." *Econometrica*, 57(4): 937.

Ghil, Michael, and Stephen Childress. 2011. "Topics in Geophysical Fluid Dynamics: Atmospheric Dynamics, Dynamo Theory, and Climate Dynamics."

Hambel, Christoph, Holger Kraft, and Eduardo Schwartz. 2021. "Optimal carbon abatement in a stochastic equilibrium model with climate change." *European Economic Review*, 132: 103642.

Hogg, Andrew McC. 2008. "Glacial cycles and carbon dioxide: A conceptual model." *Geophysical Research Letters*, 35(1).

Intergovernmental Panel On Climate Change. 2023. *Climate Change 2021 – The Physical Science Basis: Working Group I Contribution to the Sixth Assessment Report of the Intergovernmental Panel on Climate Change.* . 1 ed., Cambridge University Press.

Kriegler, Elmar, Nico Bauer, Alexander Popp, Florian Humpenöder, Marian Leimbach, Jessica Strefler, Lavinia Baumstark, Benjamin Leon Bodirsky, Jérôme Hilaire, David Klein, Ioanna Mouratiadou, Isabelle Weindl, Christoph Bertram, Jan-Philipp Dietrich, Gunnar Luderer, Michaja Pehl, Robert Pietzcker, Franziska Piontek, Hermann Lotze-Campen, Anne Biewald, Markus Bonsch, Anastasis Giannousakis, Ulrich Kreidenweis, Christoph Müller, Susanne Rolinski, Anselm Schultes, Jana Schwanitz, Miodrag Stevanovic, Katherine Calvin, Johannes Emmerling, Shinichiro Fujimori, and Ottmar Edenhofer. 2017. "Fossil-fueled development (SSP5): An energy and resource intensive scenario for the 21st century." *Global Environmental Change*, 42: 297–315.

Kushner, Harold J., and Paul Dupuis. 2001. *Numerical Methods for Stochastic Control Problems in Continuous Time.* Vol. 24 of *Stochastic Modelling and Applied Probability*, New York, NY:Springer New York.

Lontzek, Thomas S., Yongyang Cai, Kenneth L. Judd, and Timothy M. Lenton. 2015. "Stochastic integrated assessment of climate tipping points indicates the need for strict climate policy." *Nature Climate Change*, 5(5): 441–444.

Nordhaus, William D. 1992. "An optimal transition path for controlling greenhouse gases." *Science*, 258(5086): 1315–1319.

Nordhaus, William D. 2008. "A Question of Balance: Weighing the Options on Global Warming Policies."

Nordhaus, William D. 2014. "Estimates of the Social Cost of Carbon: Concepts and Results from the DICE-2013R Model and Alternative Approaches." *Journal of the Association of Environmental and Resource Economists*, 1(1): 273–312.

Nordhaus, William D. 2017. "Revisiting the social cost of carbon." *Proceedings of the National Academy of Sciences of the United States of America*, 114(7): 1518–1523.

Olijslagers, Stan, and Sweder Van Wijnbergen. 2019. "Discounting the Future: on Climate Change, Ambiguity Aversion and Epstein-Zin Preferences." *SSRN Electronic Journal*.

Pindyck, Robert S, and Neng Wang. 2013. "The Economic and Policy Consequences of Catastrophes." *American Economic Journal: Economic Policy*, 5(4): 306–339.

Sledd, Anne, and Tristan S. L'Ecuyer. 2021. "A Cloudier Picture of Ice-Albedo Feedback in CMIP6 Models." *Frontiers in Earth Science*, 9: 769844.

Taconet, Nicolas, Céline Guivarch, and Antonin Pottier. 2021. "Social Cost of Carbon under stochastic tipping points: when does risk play a role?" *Environmental and Resource Economics*, 78(4): 709–737.

Van den Bremer, Ton S., and Frederick Van der Ploeg. 2021. "The Risk-Adjusted Carbon Price." *American Economic Review*, 111(9): 2782–2810.

Weitzman, Martin L. 2012. "GHG Targets as Insurance against Catastrophic Climate Damages." *Journal of Public Economic Theory*, 14(2): 221–244.

A Steady State Density derivation

The Fokker-Planck equation for the density of temperature p is

$$\partial_T \left\{ \frac{1}{\epsilon} \mu(T, m) p(T) + \frac{\sigma_T^2}{2\varepsilon^2} p'(T) \right\} = 0, \tag{32}$$

such that, the steady state temperature $\overline{p}$ satisfies the ODE

$$\frac{1}{\epsilon} \mu(T, m) \overline{p}(T) + \frac{\sigma_T^2}{2\varepsilon^2} \overline{p}'(T) = 0, \tag{33}$$

which has solutions

$$\overline{p}(T) \propto exp\left(-\frac{V(T, m)}{\sigma_T^2 / 2\epsilon^2} \right), \tag{34}$$

where

$$\begin{aligned} V(T, m) =& (\mu_m(m) + (1 - \lambda_1) S_0) T - \frac{\eta}{5} T^5 + \\ & S_0(\lambda_1 - \lambda_2) \log(1 + \exp(T - T_i)). \end{aligned} \tag{35}$$

B Calibration

Preferences		
ρ	0.015	Discount rate
θ	10	Relative risk aversion
ψ	1.5	Elasticity of intertemporal substitution
Economy		
ω	0.002	Speed of abatement technology cost reduction
ϱ	0.0009	Growth of TFP
κ	6%32	Adjustment costs of abatement technology
δ_k	0.0116	Initial depreciation rate of capital
ξ	0.00026	Coefficient of damage function
ν	3.25	Exponent of damage function
A_0	0.113	Initial TFP
Y_0	75.8	Initial GDP
σ_k	0.0162	Variance of GDP
τ	500	Steady state horizon
Climate		
T_0	288.56	[K] Initial temperature
T^{p}	287.15	[K] Pre-industrial temperature
M_0	410	[p.p.m.] Initial carbon concentration
M^{p}	280	[p.p.m.] Pre-industrial carbon concentration
N_0	286.65543	[p.p.m.] Initial carbon in sinks
σ_T	1.5844	Volatility of temperature
S_0	342	[W / m²] Mean solar radiation
ϵ	15.844	[J / m² K year] Heat capacity of the ocean
η	$5.67e-8$	Stefan-Boltzmann constant
G_1	20.5	[W / m²] Effect of CO_2 on radiation budget
G_0	150	[W / m²] Pre-industrial GHG radiation budget
Albedo		
T_i	292.75	[K] temperature inflection point

C Motivation behind the use of Epstein-Zin preferences

Utility preferences as specified by (24) and (25) were introduced by (Epstein and Zin, 1989) (discrete time) and (Duffie and Epstein, 1992) (continuous time) to circumvent two undesirable features of additive preferences (e.g. CRRA utility) in finance. First, under additive preferences the elasticity of intertemporal substitution is the inverse of the coefficient of relative risk aversion. Second, an agent having additive preferences is indifferent between earlier or later resolution of uncertainty. Translated to the integrated models, as the one discussed in this paper, these two features yield a counter-intuitive mechanism: the abatement path becomes less ambitious as agents become more risk averse (Pindyck and Wang, 2013). This is because, in a growing economy with rising consumption, future utility decreases in risk aversion, which yields, ceteris paribus, a higher optimal emission path. The use of Epstein-Zin preferences is a common way to overcome this issue (Pindyck and Wang, 2013; Crost and Traeger, 2013; Ackerman, Stanton and Bueno, 2013; Hambel, Kraft and Schwartz, 2021; Olijslagers and Van Wijnbergen, 2019).

To make sense of this utility specification it is useful to consider two illustrative parameter cases. First, as the elasticity of intertemporal substitution converges to the inverse coefficient of relative risk aversion, $\psi \to 1/\theta$, the aggregator (25) becomes separable

$$\lim_{\psi \to 1/\theta} f(C,U) = \rho \left(\frac{1}{1-\theta} C^{1-\theta} - U \right), \tag{36}$$

and the utility (24) simplifies to the usual time separable formulation

$$U(\alpha,\chi) = \rho\, \mathbb{E} \int_t^\infty \exp\big(-\rho(s-t) \big)\, \frac{1}{1-\theta} C(s)^{1-\theta}\, \mathrm{d}t. \tag{37}$$

Second, if we let the elasticity of intertemporal substitution converge to one, $\psi \to 1$, we obtain the log-separable aggregator

$$f(C,U) = \rho(1-\theta)U \left(\log(C) - \frac{1}{1-\theta} \log\big((1-\theta)U\big) \right). \tag{38}$$

D Simplifying Assumptions

For computational purposes, it is convenient to make some simplifying assumption to reduce the dimensionality of the state space.

D.1 Decay Rate of Carbon

The calibrated carbon decay δ_m, as a function of the carbon stored in sinks N, is illustrated in Figure (10). The calibration assumes a functional form

$$\delta_m(N) = a_\delta e^{-\left(\frac{N-c_\delta}{b_\delta}\right)^2}, \tag{39}$$

for parameters $a_\delta, b_\delta, c_\delta$.

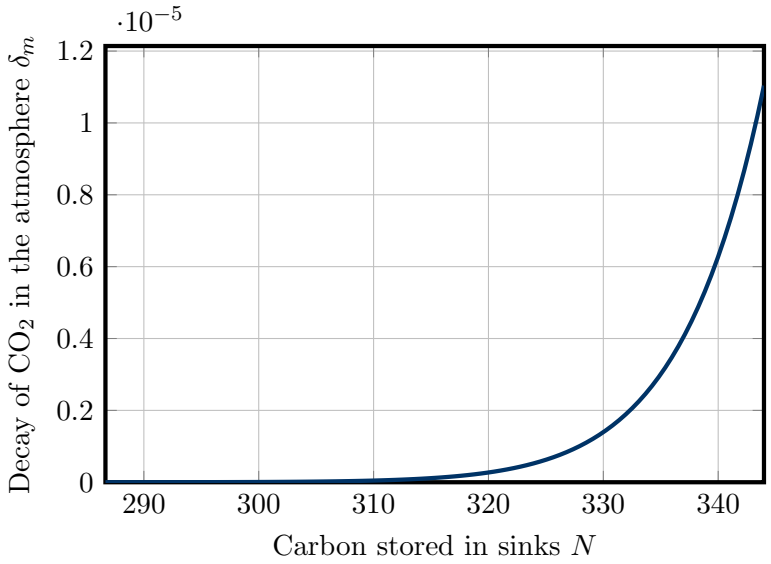

Figure 10: Estimated decay of carbon δ_m as a function of the carbon stored in sinks N.

To simplify matters I will assume that the amount of carbon sinks present in the atmosphere is a constant fraction of the concentration in the atmosphere, $N = \frac{N_0}{M_0} M$. Using this setup, under a business-as-usual emission scenario, the decay of carbon follows the path in Figure 11.

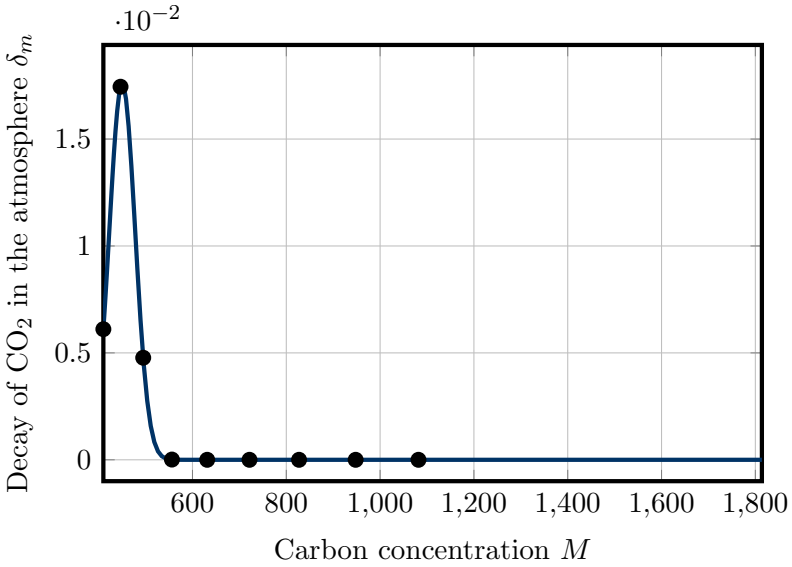

Figure 11: Estimated decay of carbon δ_m under the business as usual emission scenario M^{b}. Each marker is the decay after every decade.

E Approximating Markov Chain

Th numerical method employed here adapts that presented in (Kushner and Dupuis, 2001). First, we define a suitably large domain for the state variables $\mathcal{X} \subseteq \mathbb{R}^3$ and let $x = (T, m, y) \in \mathcal{X}$ be the state vector. Then, let $u = (\chi, \alpha) \in \mathcal{U} \coloneqq [0,1] \times [0, \gamma^{\text{b}}]$ be the vector of controls. Then we can define the operator

$$\begin{aligned}\mathcal{L}_t^u = \frac{\mu(T,m)}{\epsilon}\frac{\partial}{\partial T} + \big(\varrho + \phi(\chi) - \delta_k - d(T) - A\beta(\alpha)\big)\frac{\partial}{\partial y} + \\ (\gamma^{\text{b}} - \alpha)\frac{\partial}{\partial m} + \frac{(\sigma_T/\epsilon)^2}{2}\frac{\partial^2}{\partial T^2} + \frac{\sigma_k^2}{2}\frac{\partial^2}{\partial y^2}\end{aligned} \tag{40}$$

such that the value functional at time t satisfies

$$-\partial_t V_t = \sup_u \ \mathcal{L}_t^u V_t + f(\chi, y, V_t). \tag{41}$$

We seek to define a Markov chain consistent with (41), over a finite grid in the unit cube

$$\Omega_h = \{0, h, 2h \dots 1-h, 1\}^3. \tag{42}$$

First we define the state dynamics over the unit cube by letting $\tilde{X} = X/|\mathcal{X}|$ where

$$\mathcal{X} = [T^p, T^p + \Delta T] \times [m_0, \overline{m}] \times [y_0, \overline{y}] \tag{43}$$

and defining the dynamics

$$d\tilde{X} = \omega(t, X, u)\ \mathrm{d}t + \Sigma\ \mathrm{d}w \tag{44}$$

where

$$\omega(t, X, u) = \begin{pmatrix} \mu(T, m)/\epsilon\Delta T \\ (\gamma^{\mathrm{b}} - \alpha)/(\overline{m} - m_0) \\ \big(\varrho + \phi(\chi) - \delta_k - d(T) - A\beta(\alpha)\big)/(\overline{y} - y_0) \end{pmatrix} \tag{45}$$

and

$$\Sigma = \begin{pmatrix} \sigma_T/\epsilon\Delta T & 0 & 0 \\ 0 & 0 & 0 \\ 0 & 0 & \sigma_K/(\overline{y} - y_0) \end{pmatrix}. \tag{46}$$

For a given state X_i we can now define the transition probabilities. Let

$$Q(X_i) = \left(\frac{\sigma_T}{\epsilon\Delta T}\right)^2 + \left(\frac{\sigma_K}{\overline{y} - y_0}\right)^2 + h \max_u |\omega(t, X_i, u)| \tag{47}$$

then

$$p(X_i, X_i \pm h\Delta T) = \frac{\frac{\sigma_T^2}{2(\epsilon\Delta T)^2} + h\ \omega_T^{\pm}(t, X_i, u)}{Q(X_i)}. \tag{48}$$

Finally, let

$$V^h(t, X) = \sum_{\tilde{X}} p(X, \tilde{X}) V^h(\tilde{X}) + \frac{1}{1-\theta}\left(e^{-\rho\Delta t}((1-\theta)V^h(t, X))^{\frac{1-1/\psi}{1-\theta}} + \Delta t C^{1-\frac{1}{\psi}}\right)^{\frac{1-\theta}{1-1/\psi}}. \tag{49}$$

(Kushner and Dupuis, 2001) have shown that the transitional probabilities p form a consistent Markov chain and that $V^h \to V$ as $h \to 0$.

F Post-transition phase

We assume that at some point in the future $\tau \gg 0$, the abatement rate is equal to emission growth, $\gamma^b = \alpha$, and technological progress caps, $\varrho = 0$, such that the state variables evolve according to dynamics

$$\mathrm{d}m = 0, \tag{50}$$

$$\epsilon\ \mathrm{d}T = \mu(T, m)\ \mathrm{d}t + \sigma_T\ \mathrm{d}w_1 \text{ and} \tag{51}$$

$$\mathrm{d}y = \big(\phi(\chi) - \delta_k^p - d(T)\big)\ \mathrm{d}t + \sigma_k\ dw_2. \tag{52}$$

I call this the *post-transition* phase. We can then compute a steady state value function $V_t =: \overline{V}$ for all $t \geq \tau$, which satisfies the Hamilton-Bellman-Jacobi equation

$$0 = \overline{\mathcal{L}}^{\chi} \, \overline{V} + f(\chi, y, \overline{V}), \tag{53}$$

where

$$\overline{\mathcal{L}}^{\chi} = \frac{\mu(T,m)}{\epsilon} \frac{\partial}{\partial T} + \Big(\phi(\chi) - \delta_k - d(T)\Big) \frac{\partial}{\partial y} + \frac{(\sigma_T/\epsilon)^2}{2} \frac{\partial^2}{\partial T^2} + \frac{\sigma_k^2}{2} \frac{\partial^2}{\partial y^2}. \tag{54}$$